Path to Diversity and to Resistant Uniformity: Intracellular Adaptation to Nutrient Environment

Victoria Korogodina (korogod@jinr.ru)
Joint Institute for Nuclear Research

Research Article

Keywords: intracellular adaptation, variability and resistant uniformity, protein energy and fitness landscapes, stress, yeast cells, statistical modeling

Posted Date: February 15th, 2021

DOI: https://doi.org/10.21203/rs.3.rs-153775/v1

PATH TO DIVERSITY AND TO RESISTANT UNIFORMITY: INTRACELLULAR ADAPTATION TO NUTRIENT ENVIRONMENT

Victoria L. Korogodina [1,*]

[1]Joint Institute for Nuclear Research, Laboratory of Radiation Biology, Dubna, Moscow region, 141980, Russia

[*] korogod@jinr.ru

ABSTRACT

Two adaptation strategies are known, which provide variability and resistance of population. We study the laws of adaptation by the example of proteins and changes in their conformations. The data were obtained in the experiments of V.I. Korogodin on yeast cells with mutations, which have demonstrated the effect of the culture medium on the appearance frequency of pseudo-wild type cells. Here, these archived and published data are analyzed by the statistical approach. Statistical analysis shows the emergence of a sequence of independent foci of the pseudo-wild cells induced by intracellular factor and their association with the cytosolic and nuclear-mitochondrial oxidative pathways; the foci dispersions conform the regularities of the folding energy landscape; intracellular imbalances and gene mutations affect their frequency and diversity. We conclude that the paths from diversity to uniformity of protein conformations obeys the laws of the energy landscape. The nuclear-mitochondrial machinery generates new proteins and their homogeneous foci. Variable foci consist mainly of the former conformations remodeled under ROS from several cytosolic sources. Strong gene expression induces oxidative stress, which increases the frequency of homogeneous conformations and reduces variability. Further, stress activates a new focus of new homogeneous conformations.

Keywords: intracellular adaptation, variability and resistant uniformity, protein energy and fitness landscapes, stress, yeast cells, statistical modeling

INTRODUCTION

In the mid-1980s, V.I. Korogodin and his colleagues examined the hypothesis that functional activity of genes increases their mutation frequency [1, 2]. Scientists tested the "reversion frequency" of auxotrophic haploid yeast cells under starvation. The studies showed that adenine or leucine starvation increases occurrence frequency of pseudo-wild type cells (PWTC) in yeast with missense [2] and nonsense [3] mutations, but to a different extent. The authors explained this phenomenon by increased gene mutagenesis caused by changing of the conformation of functioning genes [2], which is becoming more accessible to the intracellular influences [4].

In the last two decades, another adaptation pathway has been intensively studied, which is associated with the conformational variability of proteins [5]. The protein three-dimensional (3D) structure is considered from the point of view of folding energy landscape [6, 7] formed under intracellular environment [8]. The proteins have to be optimized to attain a defined 3D structure, which should be in agreement with its nature state and compatible with intracellular ensemble of physical, chemical and biological conditions [8, 9]. Optimized protein conformation has the adapted phenotype.

In eukaryotic cells, the adaptation processes are linked with the reactive oxidative species (ROS) pathways [10, 11]. The ROS produced by ionizing and UV irradiation and direct treatment of cells by oxidants induce direct damage to DNA/protein/lipids [11]; high level of ROS can induce chromosomal rearrangements and cell death [12]. The ROS influence molecular chaperone activity [13], induce signaling to proliferation/differentiation, apoptosis [11], autophagy [14], and gene expression [15]. The main adaptive function of ROS is their influence on protein folding [16, 17] and activation of the unfolded protein response (UPR) [18] in the endoplasmic reticulum (ER).

Nutrient imbalance influences the ROS level and protein folding. Starvation induces peroxidation of membrane lipid of eukaryotic cells [19, 20], which results in the cytosol oxidation and causes the gene expression [15] together with mitochondrial ROS [11]. Cytosolic and nuclear-mitochondrial ROS promote ER oxidation [17]. The ER oxidizing supports the formation of intra- and interchain disulfide bonds that serve to stabilize the protein folding [16]. In their turn, formation of each disulfide bond during oxidative folding produces a single ROS [16]. The UPR activates the adaptive signaling pathways to provide an efficient protein-folding environment [18]. Nutrient-rich conditions activate the eukaryotic target of rapamycin (TOR) complex1 that promotes cell growth [21, 22, 23]. The intracellular ROS production caused mainly by mitochondrial respiration and, to a lesser extent, through NADPh oxidase [24, 25]. Redox conditions regulate protein folding, vacuolar autophagy and mitochondrial functions [26, 27].

Gene mutations change the protein folding. Missense mutation results in an altered DNA codon that shifts the equilibrium between different conformational substates [28] resulted in a prolonged obtaining of functioning conformation [29]. The study of the misfolded proteins demonstrate a reduction of interaction with chaperones [29, 30],

instability and degradation of their structure [31, 32] resulting in a strong ER stress [30]. It can affect the flexibility of the protein molecule [33, 34]. Nonsense mutation results in a premature stop codon in the transcribed mRNA. The heritable factor [PSI+] appears when the SUP35 gene is expressed and causes mistranslation [35, 36]. Sup35p is capable of adopting an aberrant conformation, which manifests as the prion-associated phenotype [37]. Sup35p possess a conserved N-terminal domain [38], which determines the physical specificity of structural variants of yeast prions, to which the chaperone machinery must conform [39, 40]. In this way, translation termination efficiency is regulated through a prion-mediated mechanism that demonstrates its important part in adaptation [41, 42, 43].

This investigation focuses on the processes of adaptation to nutrient media in cells of yeast *Saccharomyces cerevisiae* with missense ade2-192 and nonsense leu2-1 mutations. Regression analysis shows that adaptation results in an occurrence of the time-separated foci of PWTC colonies, and sequence of the PWTC foci detects specific structure of the folding energy landscape. This suggests that the PWTC foci correspond to a set of variants of protein conformation. Statistical approach reveals the adaptation regularities: nutrient imbalance increases the PWTC production; variable cytosol oxidation provides diversity of the PWTC foci, and nuclear-mitochondrial machinery generates homogeneous conformations; missense and nonsense mutations demonstrate different relationship between variability and resistant uniformity. Stationary phase and prolonged stress decrease conformational variability, and increase possibility of generation of new foci associated with gene expression.

RESULTS

Foci of the PWTC occurrence. Here, the numbers of *L*- and *S*- PWTC' colonies (Tables S1, S2) are analyzed depending on their appearance in time. The model of a single Gaussian or lognormal peak doesn't satisfy the statistical Kolmogorov-Smirnov' [44] and χ^2 criteria ($\approx 100 - 1000$). Approximation of the experimental data by the composition model consisting of the complex of several lognormal functions satisfies the statistical criteria very well (Fig. 1). The composition model suggests that the revealed effects do not exceed the intracellular interactions. The single-peak distribution can be observed when an external source is irradiation or the chemical oxidants in cell culture that can cause DNA damages [11, 45].

ROS generation is the time-dependent intracellular factor, which determines cell paths including protein folding [11, 46] both under stress and in normal conditions (Fig. 1). Difference of foci indicates different ROS pathways influencing the 3D protein structure. The PWTC occurrence can be result of ROS-depended protein misfolding [18, 17]. Let's take this assumption as a working hypothesis.

Two pathways of protein misfolding. The PWTC can be divided into two groups (Fig. 1). The efficiency of the composition of two lognormal functions is greater than that of a single-peak model (χ^2-criterion is 10 – 100 times better), but worse than the several foci model.

The correlation analysis demonstrates different character of relationships between the averaged values $\overline{N}\ (I)$, $\overline{N}\ (II)$ and the initial conditions. In yeast a *leu2-1 lys1-1*, the dependence of the first *L*- group on the leucine content is nonlinear ($R_1 = 0.3051$) and it is negative and close to linear in the second *L*- group ($R_2 = -0.9996$). The partial correlation coefficient between *L*- groups is very small ($r_{1,2} = -0.0262$). The first and second *S*-groups are highly correlated ($r_{1,2} = 0.9992$). In yeast a *ade2*-192, the enlarged volume of the medium slightly increases the first *L*-group and decreases the second one; it means that the *L*-groups are generated by different mechanisms. *S*-groups are small.

The ROS production is associated with the cytosolic sources and substantially with the mitochondria [11, 25]. Thus, the larger second group is associated with the nuclear-mitochondrial machinery. In the case of the S- genes, leucine content influences the cells as a whole; therefore both groups are minimal at low leucine content, and increase at extracellular leucine. The medium volume influences the groups, because metabolism depends on carbon sources [47]. Two pathways of ROS production and protein misfolding are presented in the scheme (Fig. 2).

Under starvation, the first group (*dotted line*) is associated with cytosol oxidation through membrane lipid peroxidation [19]. The second group (*solid line*) is shifted in time because it is linked with gene expression (*nucleus*) stimulated by cytosol oxidation [15, 11] that is accompanied by the respiration (*mitochondrion*) and ROS production [11]. Missense mutation increases strongly gene expression, ROS production, and ER stress [30]; nonsense mutation causes [PSI+] appearance, which induces mistranslation [35].

Nutrient-rich media induce occurrence of the first group (*dotted line*) mainly through NADPh formation [25] in mitochondrial chain (*mitochondrion*). The second group (*solid line*) is linked with activation of conserved in eukaryotes *TOR complex1*, which controls cell growth [21]. Cell reproduction stimulates mitochondrial respiration (*mitochondrion*) and ROS production [25]. This pathway contributes heavily into ER oxidation.

The first pathway is associated with degrading and remodeling of the previous protein conformations, and the second includes generation and folding of the new protein structures. These paths need different time and form

two separate groups of the PWTC focuses. Appearing of the misfolded proteins associated with S- genes is consistent with the similar scheme.

The frequency of PWTC colonies. The fitness of organisms to environmental conditions is described by fitness landscapes that take into account positive and negative selection [48]. Fig. 3 presents the occurrence frequency of PWTC colonies for strains a *leu2-1 lys1-1* (Table S1) and a *ade2-192* (Table S3). It describes the fitness landscapes because PWTC multiplication and formation of their colonies (Table S1, S3) depend on the appropriate nutrient conditions. The stress-induced landscape is small but frequency is high due to the strong gene expression and the large amount of ROS; landscapes generated by standard and rich media increase due to the contribution of cytosolic PWTC, but their frequency is lower.

In cells a *leu2-1 lys1-1*, the PWTC frequencies differ not significantly by transferring from the standard and rich MM conditions to the SM (Fig. 3a, b) due to nonsense suppression. However, starvation stress increases PWTC frequency. Yeast cells a *ade2-192* with missense mutation causes much higher *L*- PWTC frequency by transferring from the standard and rich medium to the SM conditions than at starvation (Fig. 3e, f). It is explained by the fact that stress induces strong degradation of the cytosolic group. The *S*- PWTC frequency increases on the SM and in general obeys the similar regularities (Fig. 3c - h).

Variability and resistance of the PWTC. The adaptation process provides the survival of population through its diversity and its resistance to the environment conditions. Protein structure gets these properties during its folding described by energy landscape [49, 6]. Conformational substates are associated with local minima of the energy landscape. The density of the minima increases exponentially with the energy [50]. Each minimum is characterized by the potential and vibration free energies, which are highly correlated [51]. The free energy specifies minima and influences the foci dispersions. In this way, the PWTC foci with different dispersions determine variability of the conformational substates. Approximation to the native state minimizes free energy of 3D protein structure, focus dispersion and PWTC variability. Fig. 4 presents *L*- and *S*- foci dispersions in dependence on their index number.

The cytosolic group is generated by several mechanisms of ROS production and consists of different large PWTC foci, which decrease with their index number. Excessive levels of the limiting metabolite (Fig. 4c) and a large volume of nutrient medium (Fig. 4d) do not increase variability. The nuclear-mitochondrial mechanisms generate ROS evenly and permanently; therefore, dispersion and variability of PWTC foci are small. High gene expression increases ROS level that decreases cytosolic group due to degradation of unusable conformations. Long-term oxidative stress select single foci, whose resistance increases due to appearance of hidden substates provided interaction with certain environmental substrates [51]. Fig. 4a shows that the more expressed *L*- genes correspond to the smaller variable cytosolic groups.

Specificity of nonsense and missense mutations. In the case of nonsense mutation, a low-energy barrier between misfolded and natural protein variants creates a high probability of the different protein conformations [50]. The first foci group demonstrates several large dispersions (Fig. 4a) that means high variability [52]. The hidden protein variants are also exposed [5, 53]. The foci of the second group are induced due to nuclear-mitochondrial machinery; their dispersions are small and hardly differ (Fig. 4a, c).

In the case of missense mutation, the formation of protein 3D structure requires strong gene expression to select rare stable protein conformation [54]. Due to strong ER stress, the cytosolic group has lost the first PWTC foci together with their diversity (Fig. 4b, d). Fig. 4d shows that *L*- and *S*- foci diversity depends directly on operation of the nuclear-mitochondrial machinery. Experiments with different volumes of nutrient medium show that low volume 10 ml reduced mRNA production and the nuclear-mitochondrial group, but the cytosolic group increased due to slight ROS in comparison with the standard volume 30 ml.

Fig. 5 shows resistance and variability of appearance frequency in the foci of *L*-PWTC. Nonsense mutation stimulates variability of cytosolic group on both minimal (MM, exp) and selective (SM, exp) media in exponential phase; aging (SM, stat) reduces cytosolic PWTC frequency and variability. The stable nuclear-mitochondrial group decreases a little in the stationary phase (SM, stat). Cells with a missense mutation produce mostly nuclear-mitochondrial PWTC, which are single on minimal media and multiply on selective media. These foci are resistant and enlarge (Fig. 5).

DISCUSSION

Experimental data and regression analysis revealed a set of time-separated foci of the PWTC colonies (Fig. 1), which are produced by an intracellular mechanisms, because an extracellular factor induces gene damages [11] described by a one-humped distribution [45]. This is the basis for the hypothesis that the reason for PWTC diversity is the variability

of the 3D protein conformations. This hypothesis is clearly confirmed by the regularities of the foci dispersions (Fig. 5), which demonstrate the laws of the energy landscape of protein folding [6].

The foci of misfolded proteins form two groups (Fig. 1). The first cytosolic group produces diversity associated with different sources of ROS, which induce degradation and remodeling of the earlier protein conformations (Fig. 2). The second group is associated with permanent operation of nuclear-mitochondrial machinery. This group produces uniform resistant PWTC foci, their diversity is small (Fig. 4).

The changes of protein conformations depend on the intracellular imbalance (Fig. 2). Stress influences both PWTC groups. The stronger the stress, the higher the frequency of PWTC (Fig. 3) induced by high gene expression. The same reason increases mitochondrial ROS production, which decreases diversity of PWTC foci (Fig. 4) caused by degradation of some conformations of the cytosolic group. Stress is a factor, which reduces the variability of the 3D protein structure and increases uniformly stable nuclear-mitochondrial group. However, the stress-induced environment modifications can cause an appearance of a new focus in the nuclear-mitochondrial group (Fig. 5). Over-rich environment does not influence the variability (Fig. 4) and PWTC frequency (Fig. 3) in comparison with the standard conditions.

Gene mutations effect on the adaptation pathway differently. Nonsense mutations trigger a mechanism of nonsense suppression [35], therefore the PWTC frequency coincides practically on the minimal and selective media (Fig. 3a, b). The cytosolic group contributes into PWTC variability (Fig. 4a, c); the nuclear-mitochondrial group increases homogeneous stable PWTC frequency (Fig. 3a). Variability of protein conformations is described in [37, 42, 39]. Missense mutation induces instability and overexpression of gene to get stable protein conformation [31]. Instability reduces strongly the cytosolic PWTS group; the nuclear-mitochondrial group has small variations (Fig. 4d). Missense mutation increases resistance [34, 28].

In 1967, the theory of r/K-selection was published [55], which had described quality and quantity strategies of adaptation. In proteins, the adaptation process is associated with their three-dimensional structures (Fig. 1). Fig. 5 illustrates regularities of intracellular adaptation process in cells with missense and nonsense mutations, variability and resistance of the *L*-PWTC foci. Prolonged stress and stationary phase decrease the number and diversity of cytosolic groups. Nuclear-mitochondrial group is stable and uniform, but splits out two or three subgroups under prolonged stress or aging, which change intracellular environment.

External sources induce like scheme of adaptation [45, 56]. For example, radiation induces mutations, which divide the population into two subpopulations, - sensitive variable and resistant ones; prolonged radiation and aging stimulate appearance of new subpopulations. This scheme is general in nature.

CONCLUSIONS

The transition from diversity to uniformity of protein conformations obeys the laws of the energy landscape of protein folding. The changing intracellular environment and genetic disorders adjust the energy landscape and thereby affect the variability of protein conformations. These factors influence two paths of the protein population to variability and uniform resistance. The nuclear-mitochondrial path generates new proteins and homogeneous conformations in the uniform foci. Variable foci consist mainly of the former conformations that remodeled due to ROS from several sources in the cytosolic path. Strong gene expression induces heavily oxidative stress, which increases the frequency of homogeneous protein conformations and reduces variability. Moreover, stress induces the formation of a new focus of new homogeneous conformations.

MATERIALS AND METHODS

Strains. The experimental data were obtained in the investigations of V.I. Korogodin [1, 2, 3]. In these experiments, we used haploid auxotrophic strains of the yeast *Saccharomyces cerevisiae*: a *ade2-192*; a *ade2*-192 *lys5-3*; a *ade2-192 lys5-3*; a *leu2-1lysl-1*. Mutation ade2-192 is missense, whereas leu2-1 and lys1-1 are ochre nonsense mutations.

Differentiation and calculation of the PWTC. Yeast cells were seeded on minimal salt medium (MM), then the grown colonies were smeared and transferred to selective medium (SM) for a given time intervals. The worked methods [2] made it possible to separate the PWTC emerged on the MM and the SM condition. The PWTC were differentiated as "locus" (*L*) and "suppressor" (*S*) ones [57]. This was checked by phenotypic analysis consisting of the determination of the biochemical requirements of the PWTC. In the case of Ade^+ PWTC, the color of the colonies can be used to differentiate *L*- and *S*-type of PWTC [58]. Frequency of the PWTC occurrence was calculated by the formula $R = \left(\frac{1}{n}\right) * ln\left(\frac{N_0}{N_0 - N}\right)$, where n is number of cells in the colonies (or the increase of the number of cells in the colony during residual growth), N_0 is general number of colonies, and N is number of PWTC colonies.

Experimental data and statistics. The experiments with different concentrations of leucine (C_{leu}) and adenine (C_{ade})

are published [2, 3], and archival material is presented in the Tables S1; S3. Unpublished archived data (Table S2) show the dependence of the occurrence of Ade$^+$ PWTC on different volumes of medium. The errors in estimating the number of PWTC colonies were 10-12%. PWTC frequency estimation errors were 10-15%.

Statistical approach. A statistical approach was used to study the regularities of PWTC occurrence. The lognormal law effectively describes the division/reproduction processes [59]. This model is presented here, although the Gaussian and geometric laws were examined too. Scientific data analysis and graphing were performed by SigmaPlot13 package. The experimental data were described by the sum of lognormal distributions: $N(k) = \sum_{i=1,k} \frac{A_i}{\sqrt{2\pi}\sigma_i x} exp\left(-\frac{(ln\frac{x}{\mu_i})^2}{2\sigma_i{}^2}\right)$, where $N(k)$ is the number of the PWTCs identified in the k foci; A_i is the value of the i-th focus, and μ_i and σ_i are the parameters of the lognormal distributions. The verification of the fitting efficiency was fulfilled using the Kolmogorov-Smirnov (KS) test [44] and χ^2 – criteria [60].

Correlation analysis. All PWTCs determined in the $i = 1,2...m$ foci (Fig. 1) are divided into two groups. The correlation analysis reveals specific links of these groups with intracellular conditions and between each other. Both groups are presented by the averaged values $\overline{N}(I) = \frac{1}{m}\sum_i N_i(I)$ and $\overline{N}(II) = \frac{1}{m}\sum_i N_i(II)$. For the leu2-1 mutation, the averaged values $\overline{N}(I)$ and $\overline{N}(II)$ take into account the MM and SM conditions in the exponential and stationary phases: MM, exp; SM, exp; MM, stat; SM, stat. For the ade2-192 mutation, the averaged values were calculated in the conditions SM, exp; SM, stat. Correlation analysis will reveal dependence of the $\overline{N}(I)$ and $\overline{N}(II)$ on the nutrient medium and between these groups. The correlation coefficients were determined by the standard formulas [60].

Estimation of the foci dispersions. The foci dispersions $\overline{\sigma_i}(L)$ and $\overline{\sigma_i}(S)$ (Fig. 4a, b) were estimated in the exponential phase as averaged values over three nutrient media C_{leu} = 3, 30, 300 mg/l in the MM and SM conditions (a) and over two volumes of medium V_{MM} = 10, 30 ml/dish in the SM conditions (b). The foci dispersions $\overline{\sigma_i}(L)$ (Fig. 4c, d) were determined for three initial leucine concentrations C_{leu} = 3; 30; 300 mg/l, each of them were averaged over the MM and SM conditions in the exponential and stationary phases (c), and for two volumes V_{MM} = 10, 30 ml/dish in the SM conditions (d).

Acknowledgement. This investigation is dedicated to Prof. V.I. Korogodin, who started these investigations. I am grateful to our colleagues N.A. Koltovaya, O.V. Komova, E. Dushanov, A.N. Bugay for discussions, and especially thanks to Profs. G.A. Ososkov, V.A. Nikitin, E.K. Khlestkina, T.R. Soidla, O.V. Nevzglyadova, S.G. Inge-Vechtomov, N.F. Avrova, I.V. Yekimova for their recommendations.

REFERENCES

1. Ilyina, V.L., Korogodin, V.I. & Fajszi, Cs. Dependence of spontaneous reversion frequencies in haploid yeasts of different genotypes on the concentration of adenine in the medium and on the age of the culture. *Mutat. Res. Lett*. **174**, 189-194. https://doi.org/10.1016/0165-7992(86)90149-1 (1986).
2. Korogodin, V.I. *et al*. On the dependence of spontaneous mutation rates on the functional state of genes. *Yeast* **7**, 105-117. DOI: 10.1002/yea.320070204 (1991).
3. Korogodina, V.L. *et al*. Characteristics of spontaneous mutagenesis in haploid yeasts. *Yeast* **11**, 701-711. https://doi.org/10.1002/yea.320110802 (1995).
4. Gazit, B. *et al*. Active genes are sensitive to deoxyribonuclease I during metaphase. *Science* **217**, 648-650. DOI: https://doi.org/10.1126/science.6283640 (1982).
5. True, H.L. & Lindquist, S.L. A yeast prion provides a mechanism for genetic variation and phenotypic diversity. *Nature* **407**, 477-483. DOI: 10.1038/35035005 (2000).
6. Onuchic, J.N., Luthey-Schulten, Z. & Wolynes, P.G. Theory of protein folding: the energy landscape perspective. *Annu. Rev. Phys. Chem*. **48**, 545-600. DOI: 10.1146/annurev.physchem.48.1.545 (1997).
7. Chen, M. *et al*. Protein folding and structure prediction from the ground up II: *AAWSEM* for α/β proteins. *J. Phys. Chem. B* **121**, 3473–3482. DOI: 10.1021/acs.jpcb.6b09347 (2017).
8. Tavernelli, I., Cotesta, S. & Di Iorio, E.E. Protein dynamics, thermal stability, and free-energy landscapes: A molecular dynamics investigation. *Biophys. J*. **85**, 2641–2649. doi: 10.1016/S0006-3495(03)74687-6 (2003)
9. Camilloni, C. *et al*. Energy landscape of the prion protein helix 1 probed by metadynamics and NMR. *Biophys. J*. **102**, 158–167. DOI: 10.1016/j.bpj.2011.12.003 (2012).
10. Trachootham, D. *et al*. Redox regulation of cell survival. *Antioxid. Redox. Signal*. **10**, 1344-1465. http://doi.org/10.1089/ars.2007.1957 (2008).
11. Hamanaka, R.B. & Chandel, N.S. Mitochondrial reactive oxygen species regulate cellular signaling and dictate biological outcomes. *Trends Biochem. Sci*. **35**, 505–513. DOI: 10.1016/j.tibs.2010.04.002 (2010).
12. Ragu, S. *et al*. Oxygen metabolism and reactive oxygen species cause chromosomal rearrangements and cell death. *PNAS* **104**, 9747–9752. https://doi.org/10.1073/pnas.0703192104 (2007).
13. Kumsta, C. & Jakob, U. Redox-regulated chaperones. *Biochemistry* 48, 4666–4676. DOI: 10.1021/bi9003556 (2009).
14. Filomeni, G., De Zio, D. & Cecconi, F. Oxidative stress and autophagy: the clash between damage and metabolic needs. *Cell Death Differ*. **22**, 377–388. doi: 10.1038/cdd.2014.150 (2015).
15. Gasch, A.P. *et al*. Genomic expression programs in the response of yeast cells to environmental changes. Mol. Biol. Cell. **11**, 4241–4257. DOI: 10.1091/mbc.11.12.4241 (2000).
16. Shimizu, Y. & Hendershot, L.M.. Oxidative folding: cellular strategies for dealing with the resultant equimolar production of reactive oxygen species. *Antioxid. Redox. Signal*. **11**, 2317-2331. DOI: 10.1089/ars.2009.2501 (2009).
17. Cao, S.S. & Kaufman, R.J. Endoplasmic reticulum stress and oxidative stress in cell fate decision and human disease. *Antioxid. Redox. Signal*. **21**, 396-413. doi: 10.1089/ars.2014.5851 (2014).
18. Haynes, C.M., Titus, E.A. & Cooper, A.A. Degradation of misfolded proteins prevents ER-derived oxidative stress and cell death. *Mol. Cell* **15**, 767-776. https://doi.org/10.1016/j.molcel.2004.08.025 (2004).

19. Bhattacharjee, S. Membrane lipid peroxidation and its conflict of interest: the two faces of oxidative stress. *Curr. Sci*. 107, 1811-1823. https://www.jstor.org/stable/24107826 (2014).
20. Shi, K. *et al*. Reactive oxygen species-mediated cellular stress response and lipid accumulation in oleaginous microorganisms: The state of the art and future perspectives. *Front. Microbiol*. **8**, DOI: 10.3389/fmicb.2017.00793 (2017).
21. Loewith, R. 9 - TORC1 Signaling in budding yeast. *The Enzymes* **27**, 147-175. DOI: 10.1016/S1874-6047(10)27009-9 (2010).
22. Kim, S.G., Buel, G.R. & Blenis, J. Nutrient regulation of the mTOR complex 1 signaling pathway. *Mol.. Cells* **35**. 463-473. DOI: 10.1007/s10059-013-0138-2 (2013).
23. Zhenyukh, O. *et al*. High concentration of branched-chain amino acids promotes oxidative stress, inflammation and migration of human peripheral blood mononuclear cells via mTORC1 activation. *Free Radic. Biol. Med*. **104**, 165–177. DOI: 10.1016/j.freeradbiomed.2017.01.009 (2017).
24. Rich, P.R. & Maréchal, A. The mitochondrial respiratory chain**.** *Essays Biochem*. **47**, 1-23. DOI: 10.1042/bse0470001 (2010).
25. Larosa, V. & Remacle, C. Insights into the respiratory chain and oxidative stress. *Bioscience Rep*. **38**, 1-14. DOI: 10.1042/BSR20171492 (2018).
26. Lee, J., Giordano, S. & Zhang, J. Autophagy, mitochondria and oxidative stress: cross-talk and redox signaling. *Biochem. J.* **441**, 523–40. DOI: 10.1042/BJ20111451 (2012)
27. Jewell, J.L., Russell, R.C. & Guan, K-L Amino acid signalling upstream of mTOR. *Nat. Rev. Mol. Cell. Biol.* **14**, 133–139. DOI: 10.1038/nrm3522 (2013).
28. Stefl, S. *et al*. Molecular mechanisms of disease-causing missense mutations. *J. Mol. Biol*. **425**, 3919–3936. DOI: 10.1016 / j.jmb.2013.07.014 (2013).
29. Bross, P. et al. Protein misfolding and degradation in genetic diseases. *Hum. Mutat*. **14**, 186-198. DOI: 10.1002/(SICI)1098-1004(1999)14:3<186::AID-HUMU2>3.0.CO;2-J (1999)
30. Drozdova, T., Papillon, J. & Cybulsky, A.V. Nephrin missense mutations: induction of endoplasmic reticulum stress and cell surface rescue by reduction in chaperone interactions. Physiol. Rep. **1**, 1-16. DOI: 10.1002/phy2.86 (2013)
31. Gammie, A.E. *et al*. Functional characterization of pathogenic human MSH2 missense mutations in *Saccharomyces cerevisiae*. *Genetics* **177**, 707–721. doi: 10.1534/genetics.107.071084 (2007).
32. Shi, Z., Sellers, J. & Moult, J. Protein stability and *in vivo* concentration of missense mutations in phenylalanine hydroxylase. **Proteins 80**, 61–70. DOI: 10.1002/prot.23159 (2012).
33. Tang, K.E.S. & Dill, K.A. Native protein fluctuations: the conformational-motion temperature and the inverse correlation of protein flexibility with protein stability. *J. Biomol. Struct. Dyn*. **16**, 397–411. DOI:10.1080/07391102.1998.10508256 (1998).
34. Zhang, Z. *et al*. Analyzing effects of naturally occurring missense mutations. *Comput. Math. Methods. Med*. 2012. DOI: 10.1155/2012/805827 (2012).
35. Chernoff, Y.O., Derkach, I.L. & Inge-Vechtomov, S.G. Multicopy SUP35 gene induces de-novo appearance of psi-like factors in the yeast *Saccharomyces cerevisiae*. *Curr. Genet*. **24**, 268–270. DOI:10.1007/bf00351802 (1993)
36. Ter-Avanesyan, M.D. et al. The *SUP35* omnipotent suppressor gene is involved in the maintenance of the non-Mendelian determinant [*psi*+] in the yeast *Saccharomyces cerevisiae*. *Genetics* **137**, 671–676. (1994)
37. Tuite, M.F. & Lindquist, S.L. Maintenance and inheritance of yeast prions. *Trends Genet*. **12**, 467–471. DOI:10.1016/0168-9525(96)10045-7 (1996).
38. Kushnirov, V.V. *et al*. Nucleotide sequence of the SUP2 (SUP35) gene of *Saccharomyces cerevisiae*. *Gene* **66**, 45-54. https://doi.org/10.1021/bi9003556 (1988).
39. Stein, K.C. & True, H.L. Extensive diversity of prion strains is defined by differential chaperone interactions and distinct amyloidogenic regions. *PLoS. Genet.* **10**, 1-18. DOI: 10.1371/journal.pgen.1004337 (2014a).
40. Stein, K.C. & True, H.L. Structural variants of yeast prions show conformer-specific requirements for chaperone activity. *Mol. Microbiol*. **93**, 1156–1171. DOI: 10.1111/mmi.12725 (2014b)
41. Eaglestone, S.S., Cox, B.S. & Tuite, M.F. Translation termination efficiency can be regulated in *Saccharomyces cerevisiae* by environmental stress through a prion-mediated mechanism. *The EMBO J.* **18**, 1974–1981. doi: 10.1093/emboj/18.7.1974 (1999).
42. Chernoff, Y.O. Mutation processes at the protein level: is Lamarck back? *Mutat. Res*. **488**, 39–64. DOI: 10.1016/S1383-5742(00)00060-0 (2001).
43. Chernova, T.A., Wilkinson, K.D. & Chernoff, Y.O. Physiological and environmental control of yeast prions. *FEMS. Microbiol. Rev.* **38**, 326–344. DOI: 10.1111/1574-6976.12053 (2014).
44. Smirnov, N. Table for estimating the goodness of fit of empirical distributions. *Ann. Math. Stat*. **19**, 279–281. https://www.jstor.org/stable/2236278 (1948)
45. Korogodina, V.L., Florko, B.V. & Osipova, L.P. *Radiation-induced processes of adaptation: research by statistical modeling* (Springer 2013).
46. Schieber, M. & Chandel, N.S. ROS function in redox signaling and oxidative stress. *Curr. Biol*. **24**, R453–R462. DOI: 10.1016/j.cub.2014.03.034 (2014).
47. Minard, K.I. & McAlister-Henn, L. Sources of NADPH in yeast vary with carbon source. *J. Biol. Chem*. **280**, 39890–39896. DOI: 10.1074/jbc.M509461200 (2005).
48. Bazykin, G.A. Changing preferences: deformation of single position amino acid fitness landscapes and evolution of proteins. *Biol. Lett.* **11**, 20150315. http://dx.doi.org/10.1098/rsbl.2015.0315 (2015).
49. Frauenfelder, H., Sligar, S.G. & Wolynes, P.G. The energy landscapes and motions of proteins. *Science* **254**, 1598-1603. DOI: 10.1126/science.1749933 (1991).
50. Nakagawa, N. & Peyrard, M. The inherent structure landscape of a protein. *PNAS* **103**, 5279-5284. DOI: 10.1073/pnas.0600102103 (2006).
51. Ming, D., Anghelm, M. & Wall, M.E. Hidden structure in protein energy landscapes. *Phys. Rev. E*. **77**, 1-6. DOI: 10.1103/PhysRevE.77.021902 (2008).
52. Ming, D. & Wall, M.E. Interactions in native binding sites cause a large change in protein dynamics. *JMB* **358**, 213-223. DOI:10.1016/j.jmb.2006.01.097 (2006).
53. True, H.L., Berlin, I. & Lindquist, S.L. Epigenetic regulation of translation reveals hidden genetic variation to produce complex traits. *Nature* **31**, 184-187. DOI:10.1038/nature02885 (2004).
54. Goldberg, A.L. Protein degradation and protection against misfolded or damaged proteins. *Nature* **426**, 895-899. DOI:10.1038/nature02263 (2003).
55. MacArthur, R. & Wilson, E.O. *The Theory of Island Biogeography* (Princeton University Press, 1967, revised).
56. Korogodina, V.L., Grigorkina, E.B. & Osipova, L.P, Strategies of adaptation under prolonged irradiation vs chronic exposure in *Genetics, Evolution, Radiation* (eds. Korogodina, V.L. et al) 153-168 (Springer, 2016)
57. Korogodina, V.L. *et al*. Estimation of the contribution of double mutants to the observed spectrum of revertants, occurring in auxotrophic yeasts. *JINR Communications* **P19-88-835**, (1988).
58. Nevzglyadova, O.V. *et al*. Yeast red pigment modifies Amyloid beta growth in Alzheimer disease models in both *Saccharomyces cerevisiae* and *Drosophila melanogaster*. *Amyloid* **22**, 100-111. DOI: 10.3109/13506129.2015.1010038 (2015)**.**
59. Kolmogorov, A.N. About the lognormal distribution of particle sizes under fragmentation. *Bull. Acad. Sci. USSR*. **31**, 99-101. (1941).
60. Van der Waerden, B.I. Mathematische statistic. *Springer*, (1971).

LEGENDS FOR FIGURES

Figure 1. Experimental distributions of the Leu^+ [3] (a) and Ade^+ (b) PWTC occurrence in yeast a *leu2-1 lys1-1* (Table S1) and a *ade2-192* (Table S2) in time and their approximations by the composition model of several and two lognormal functions. Experimental data are presented with standard errors (SE). Regression by the n- peaks model corresponds to the Kolmogorov-Smirnov - and χ^2 -$^-$ criteria: 5%. Regression by the two- peaks model corresponds to the Kolmogorov-Smirnov criteria: 5%.

Figure 2. Two main pathways of protein misfolding under the starvation stress and in nutrient-rich conditions: cytosolic pathway through peroxidation and NADPh oxidation, nuclear-mitochondrial pathway through gene expression and mitochondrial ROS.

Figure 3. Experimental distributions of the Leu^+,[3] (Table S1) - and Ade^+ [2] (Table S3) - PWTC frequency and their approximations by the composition model of two lognormal functions. Regression curves correspond to the significance level of Kolmogorov-Smirnov- and χ^2 - criteria: 5%.

Figure 4. Dependence of foci dispersions (Fig. 1) on their index numbers approximated by the composition model of two lognormal (**a**, **b**) and two exponential (**c**, **d**) functions. The *L*- and *S*- foci dispersions (**a**, **b**) are presented in the exponential phase by their averaged values over all nutrient media. The cytosolic and nuclear-mitochondrial *L*- foci dispersions (**c**, **d**) are presented for different initial media by their averaged values in all conditions. Dispersions are shown with their root mean square errors (RMSE). Regression curves, significance level of Kolmogorov-Smirnov- and χ^2 - criteria: 5%.

Figure 5. Dependence of PWTC frequency on the nutrient medium and aging. The *L*- PWTC frequencies are presented in the different foci of their formation. The PWTC frequencies are averaged over initial leucine content (a *leu2-1lys1-1*) and over volume of medium (a *ade2-192*).

Figures

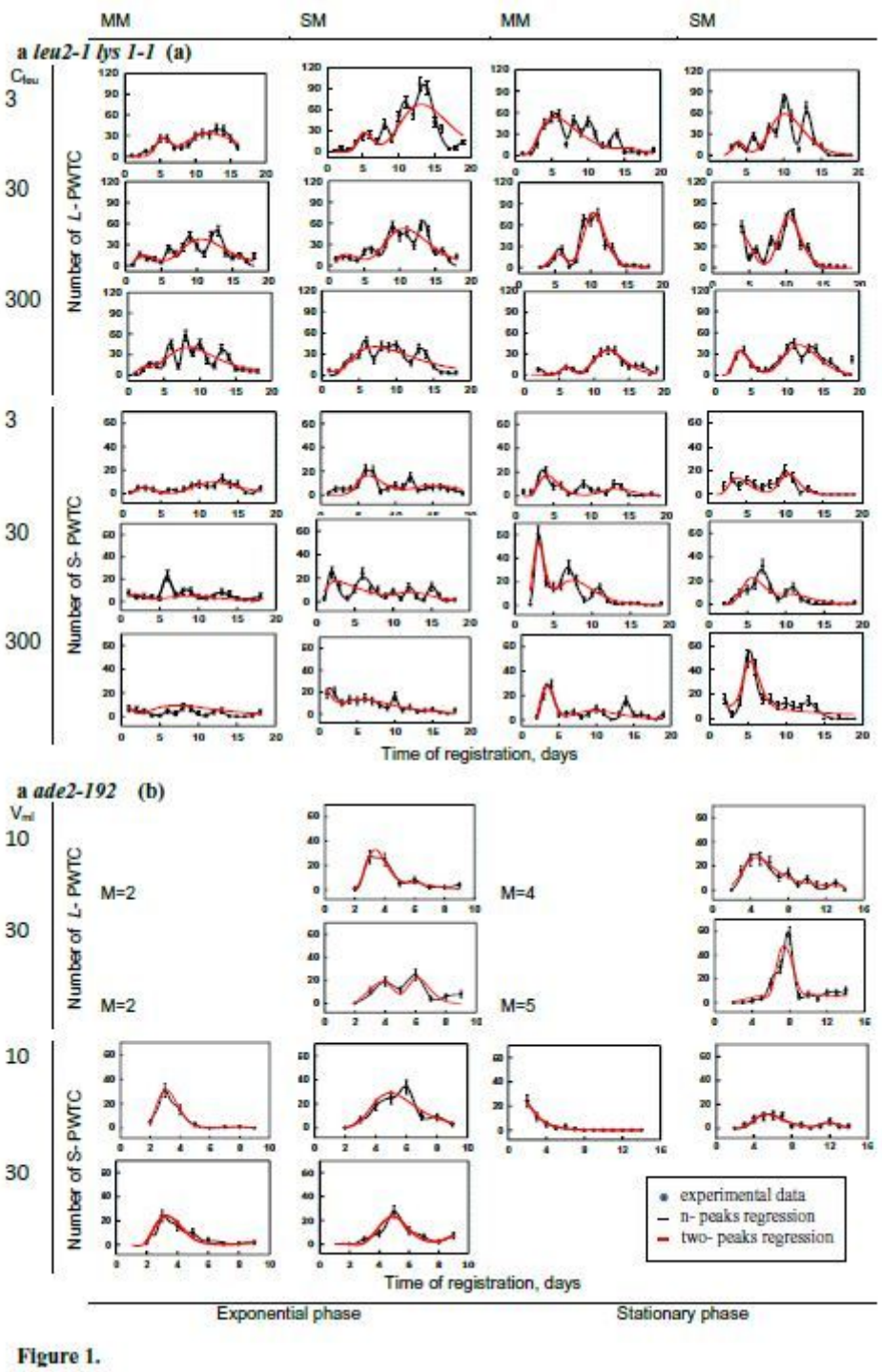

Figure 1.

Figure 1

Experimental distributions of the Leu+ 3 (a) and Ade+ (b) PWTC occurrence in yeast a leu2-1 lys1-1 (Table S1) and a ade2-192 (Table S2) in time and their approximations by the composition model of several and two lognormal functions. Experimental data are presented with standard errors (SE). Regression by the n-peaks model corresponds to the Kolmogorov-Smirnov - and $\chi 2$ – criteria: 5%. Regression by the two-peaks model corresponds to the Kolmogorov-Smirnov criteria: 5%.

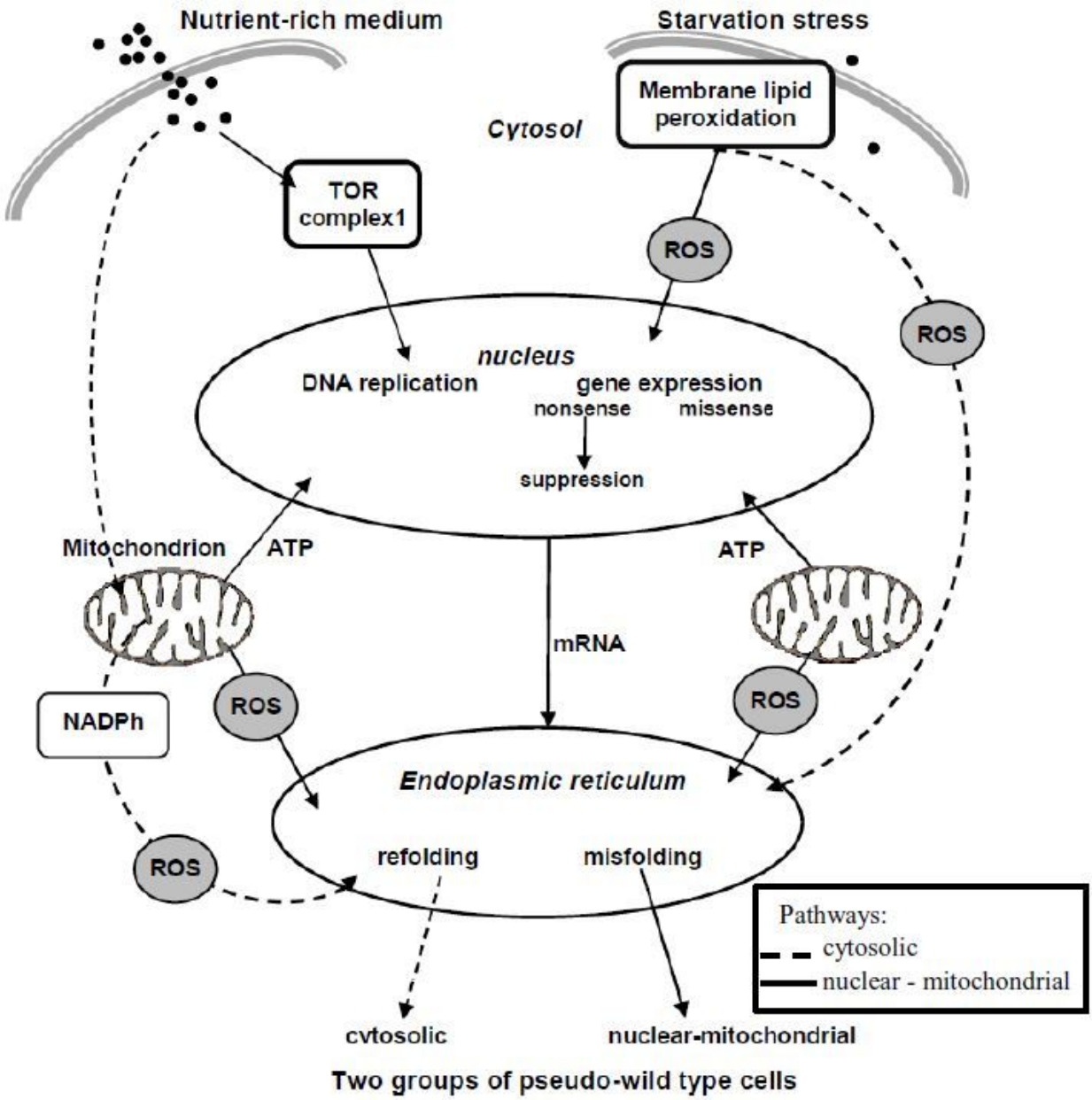

Figure 2.

Figure 2

Two main pathways of protein misfolding under the starvation stress and in nutrient-rich conditions: cytosolic pathway through peroxidation and NADPh oxidation, nuclear-mitochondrial pathway through gene expression and mitochondrial ROS.

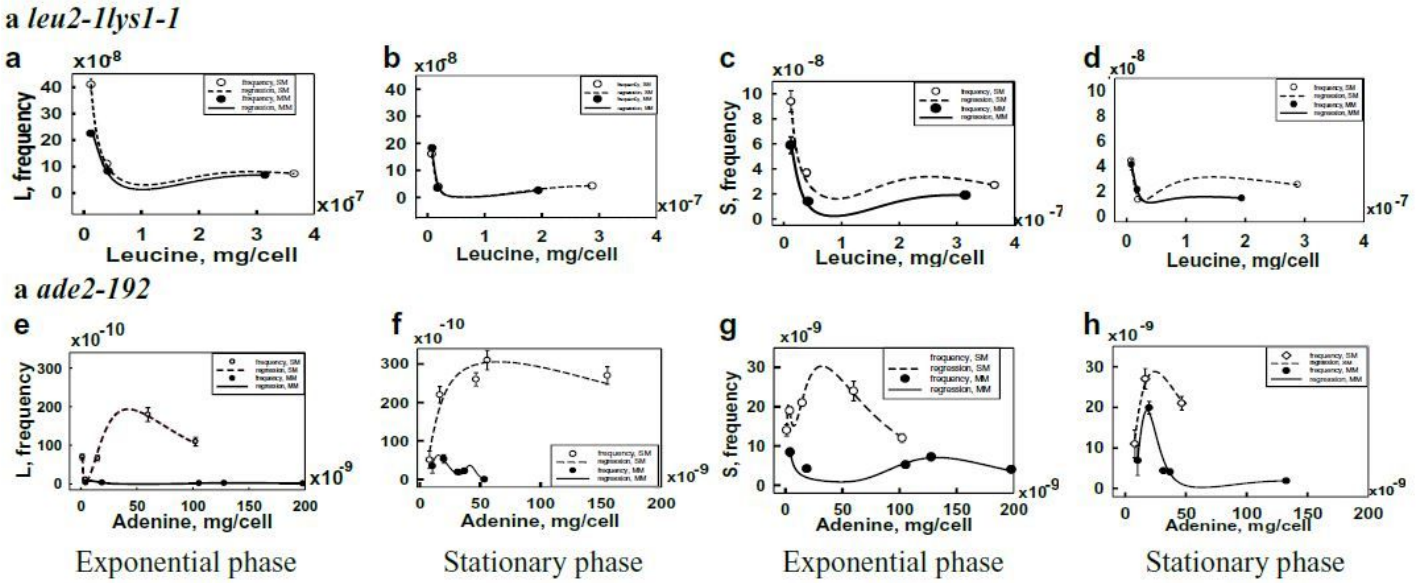

Figure 3.

Figure 3

Experimental distributions of the Leu+,3 (Table S1) - and Ade+ 2 (Table S3) - PWTC frequency and their approximations by the composition model of two lognormal functions. Regression curves correspond to the significance level of Kolmogorov-Smirnov- and χ2 - criteria: 5%.

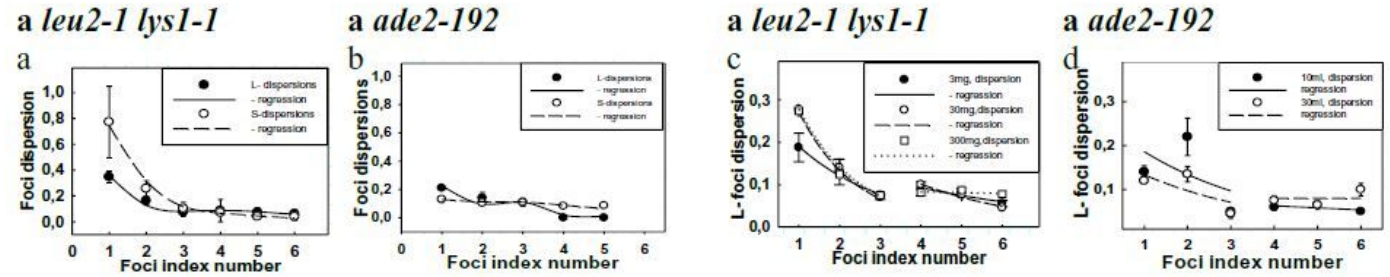

Figure 4.

Figure 4

Dependence of foci dispersions (Fig. 1) on their index numbers approximated by the composition model of two lognormal (a, b) and two exponential (c, d) functions. The L- and S- foci dispersions (a, b) are presented in the exponential phase by their averaged values over all nutrient media. The cytosolic and nuclear-mitochondrial L- foci dispersions (c, d) are presented for different initial media by their averaged values in all conditions. Dispersions are shown with their root mean square errors (RMSE). Regression curves, significance level of Kolmogorov-Smirnov- and χ2 - criteria: 5%.

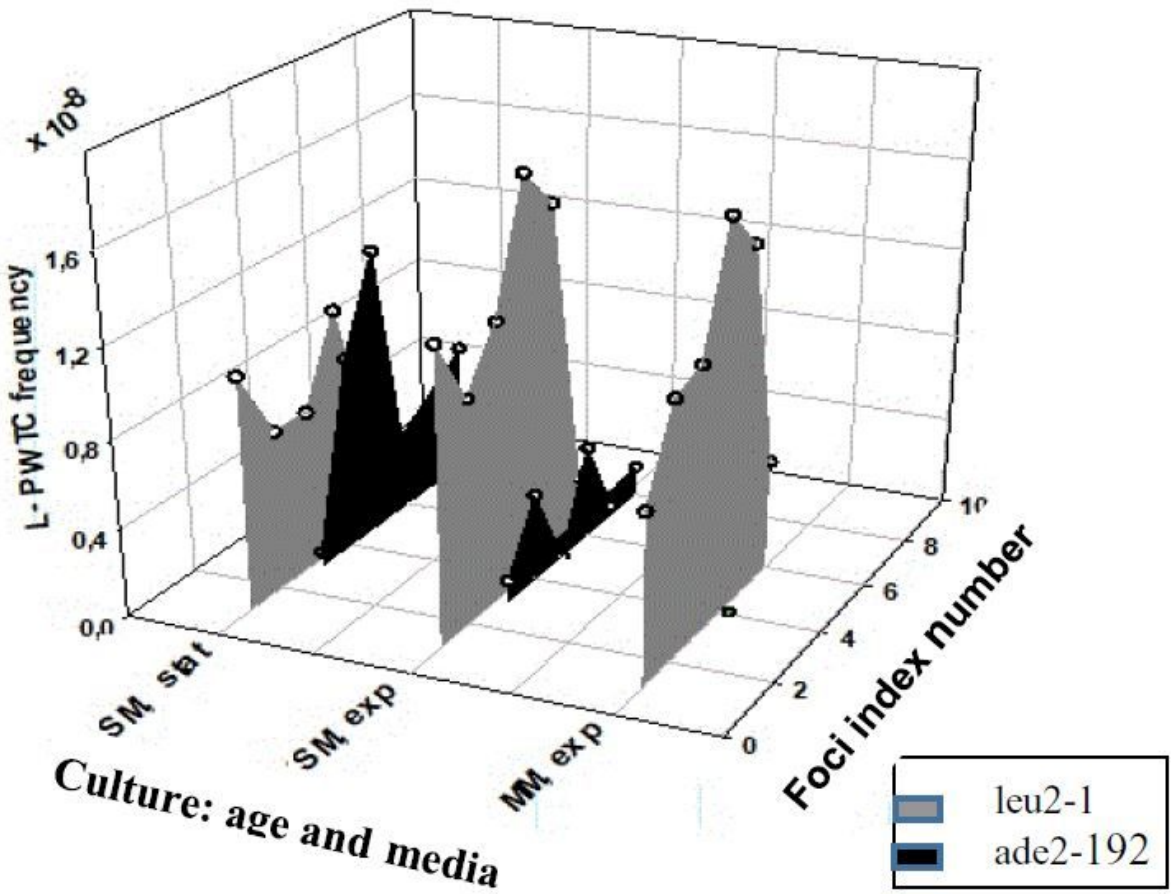

Figure 5.

Figure 5

Dependence of PWTC frequency on the nutrient medium and aging. The L- PWTC frequencies are presented in the different foci of their formation. The PWTC frequencies are averaged over initial leucine content (a leu2-1lys1-1) and over volume of medium (a ade2-192).

Supplementary Files

This is a list of supplementary files associated with this preprint. Click to download.

- Supplemetarydatasets.pdf